MOLECULAR PHYSICS REPORTS **38** (2003) 11-19

SIC-LSD DESCRIPTION OF HALF-METALLIC TRANSITION METAL OXIDES

Z. SZOTEK[1], W. M. TEMMERMAN[1], D. KÖDDERITZSCH[2], W. HERGERT[2], A. SVANE[3], L. PETIT[4], G. M. STOCKS[5], H. WINTER[6]

[1]*Daresbury Laboratory, Daresbury, Warrington WA4 4AD, UK*

[2]*Fachbereich Physik, Martin-Luther-Universität Halle-Wittenberg, Friedemann-Bach-Platz 6, D-06099 Halle, Germany*

[3]*Institute of Physics and Astronomy, University of Aarhus, DK-8000 Aarhus C, Denmark*

[4]*Computer Science and Mathematics Division, and Center for Computational Sciences, Oak Ridge National Laboratory, Oak Ridge, TN 37831, USA*

[5]*Metals and Ceramics Division, Oak Ridge National Laboratory, Oak Ridge, TN 37831, USA*

[6]*INFP, Forschungszentrum Karlsruhe GmbH, Postfach 3640, D-76021 Karlsruhe, Germany*

Abstract. We discuss the self-interaction corrected local spin density approximation (SIC-LSD) and its application to half-metallic transition metal oxides such as double perovskites and magnetite (Fe_3O_4). We concentrate on the electronic and magnetic properties of these compounds, and in addition a possible charge order in magnetite is investigated. We also show that even such simple transition metal monoxides as MnO and NiO can acquire half-metallic characteristics when doped with vacancies.

1. INTRODUCTION

The half-metallic (HM) transition metal (TM) oxides that we shall discuss can be generally referred to as half-metallic ferromagnets (HMF). The concept of a half-metallic ferromagnet was introduced by de Groot et al. [1], based on their electronic structure calculations for Heusler systems NiMnSb and PtMnSb. Half-metallic ferromagnets are solids that are metals with a Fermi surface in one spin-channel, and insulators in the other spin-channel. They give rise to 100% spin polarization, and thus may play an important role in the new field of spintronics. A broad classification scheme of half-metallic ferromagnets, encompassing localized and itinerant electron systems as well as possible semimetals and semiconductors, was proposed by Coey and Venkatesan [2] based on the electronic structure. In this paper, we shall concentrate only on two most common types of half-metallic oxides.

All half metals contain more than one element. Normal ferromagnets like Fe, Co and Ni are not half metals. Although Co and Ni have fully spin-polarized *d*-bands, with fully occupied majority spin states and only minority spin states at the Fermi level, E_F, the latter also crosses the unpolarized 4*s* band. So, there are both the spin-up and spin-down densities of states (DOS) present at E_F. Most known half metals are either oxides, sulfides, or Heusler alloys. CrO_2 is the best known oxide half metal with only spin-up electrons of mostly Cr(t_{2g}) character at the Fermi level. Another well-known half-metal of the same type (IA) is the half Heusler alloy NiMnSb, with only spin-up electrons of Ni(e_g) character at E_F. The double-perovskite Sr_2FeMoO_6 is an example of a type IB half metal [2], with no spin-up electrons at the Fermi level, but with the spin-down conduction electrons of strongly hybridized Fe($3dt_{2g}$), Mo($4dt_{2g}$) and O($2p$) character. Magnetite belongs to the type II half metals, where electrons lie in a band that is sufficiently narrow for them to be localized. The best indication of a type I or type II half metal is metallic conduction in a solid, with a spin moment at $T = 0$ which is precisely an integer number of Bohr magnetons

(μ_B) per unit cell [2]. By virtue of integer filling of one spin channel in stoichiometric half metals, the resulting spin magnetic moment per unit-cell is also integer. The integer spin moment criterion is a necessary but not a sufficient condition for half-metallicity. Spin-orbit coupling may destroy half-metallicity [3].

The question whether the total spin moment can be zero, whilst retaining half-metallicity, has been addressed first by Leuken et al. [4]. Not to be confused with usual antiferromagnets, they defined a half-metallic antiferromagnet (HMAF) as a half metal with vanishing macroscopic spin moment. Half-metallic antiferromagnets would be ideal tip materials in spin-polarized STM (SPSTM) and could have important implications for superconductivity [5]. We shall show that some vacancy doped TM oxides can become half metals, and in particular NiO with about 3% of cation vacancies is a half metal with zero spin magnetic moment, i.e., a half-metallic antiferromagnet [6].

The TM *d* electrons in half-metallic oxides are strongly correlated and cannot be adequately described within the standard band theory framework such as local spin density (LSD) approximation to density functional theory (DFT). The self-interaction corrected (SIC)-LSD [7], on the other hand, provides a better description of correlations than LSD, and was successfully applied to a variety of *d*- and *f*-electron materials [8-10]. An overview of the basic features of the SIC-LSD formalism is presented in the next section, whilst its application to double perovskites Ba_2FeMoO_6, Ca_2FeMoO_6, Sr_2FeMoO_6, and Ca_2FeReO_6, magnetite, and vacancy doped MnO and NiO, is presented and discussed in section 3. The paper is concluded in section 4.

2. THEORY

The basis of the SIC-LSD formalism is a self-interaction free total energy functional, E^{SIC}, obtained by subtracting from the LSD total energy functional, E^{LSD}, a spurious self-interaction of each occupied electron state ψ_α [11], namely

$$E^{\mathrm{SIC}} = E^{\mathrm{LSD}} - \sum_{\alpha}^{occ.} \delta_\alpha^{\mathrm{SIC}} . \tag{1}$$

Here α numbers the occupied states and the self-interaction correction for the state α is

$$\delta_\alpha^{\mathrm{SIC}} = U[n_\alpha] + E_{xc}^{\mathrm{LSD}}[\bar{n}_\alpha] , \tag{2}$$

with $U[n_\alpha]$ being the Hartree energy and $E_{xc}^{\mathrm{LSD}}[\bar{n}_\alpha]$ the LSD exchange-correlation energy for the corresponding charge density n_α and spin density $\bar{n}_\alpha$. It is the LSD approximation to the exact exchange-correlation energy functional which gives rise to the spurious self-interaction. The exact exchange-correlation energy E_{xc} has the property that for any single electron spin density, $\bar{n}_\alpha$, it cancels exactly the Hartree energy, thus

$$U[n_\alpha] + E_{xc}[\bar{n}_\alpha] = 0 . \tag{3}$$

In the LSD approximation this cancellation does not take place, and for well localized states the above sum can be substantially different than zero. For extended states in periodic solids the self-interaction vanishes.

The SIC-LSD approach can be viewed as an extension of LSD in the sense that the self-interaction correction is only finite for spatially localized states, while for Bloch-like single-particle states E^{SIC} is equal to E^{LSD}. Thus, the LSD minimum is also a local minimum of E^{SIC}. A question now arises, whether there exist other competitive minima, corresponding to a finite number of localized states, which could benefit from the self-interaction term without loosing too much of the energy associated with band formation. This is often the case for rather well localized electrons like the 3*d* electrons in transition metal oxides or the 4*f* electrons in rare earth compounds. It follows from minimization of Eq. (1) that within the SIC-LSD approach such localized electrons move in a different potential than the delocalized valence electrons which respond to the effective LSD potential. Thus, by including an explicit energy contribution for an electron to localize, the *ab initio* SIC-LSD describes both localized and delocalized electrons on an equal footing, leading to a greatly improved description of correlation effects over the LSD approximation, as well as, to determination of valence.

In order to make the connection between valence and localization more explicit, it is usefull to define the nominal valence [10] as

$$N_{val} = Z - N_{core} - N_{SIC},$$

where Z is the atomic number (26 for Fe), N_{core} is the number of core (and semi-core) electrons (18 for Fe), and N_{SIC} is the number of localized, i.e., self-interaction corrected, states (either five or six, respectively for Fe^{3+} and Fe^{2+}). Thus, in this formulation the valence is equal to the integer number of electrons available for band formation. The localized electrons do not participate in bonding. To find the nominal valence we assume various atomic configurations, consisting of different numbers of localized states, and minimize the SIC-LSD energy functional of Eq. (1) with respect to the number of localized electrons.

The SIC-LSD formalism is governed by the energetics due to the fact that for each orbital the SIC differentiates between the energy gain due to hybridization of the orbital with the valence bands and the energy gain upon localization of the orbital. Whichever wins determines if the orbital is part of the valence band or not, and in this manner also leads to the evaluation of the valence of elements involved. The SIC depends on the choice of orbitals and its value can differ substantially as a result of this. Therefore, one has to be guided by the energetics in defining the most optimally localized orbitals to determine the absolute energy minimum of the SIC-LSD energy functional. The advantage of the SIC-LSD formalism is that for such systems as transition metal oxides or rare earth compounds the lowest energy solution will describe the situation where some single-electron states may not be of Bloch-like form. Specifically, in monoxides, magnetite and double perovskites, these would be the Mn-, Ni-, and Fe-3*d* states, but not the O 2*p* or Mo 4*d* or Re 5*d* states, since treating them as localized states is energetically unfavourable.

3. RESULTS AND DISCUSSION

3. 1. Double perovskites

Interest in ordered double perovskites has started with the discovery of the room-temperature collosal magnetoresistance (CMR) in Sr_2FeMoO_6 [12]. Experimentally, half-metallic behaviour in this compound is indicated by the observed high transition temperature T_c and low field

magnetoresistance. In calculations, it is manifested through a well defined gap in the majority spin channel, and metallic behaviour in the minority spin channel, with strongly hybridized bands of Fe $3d$ (t_{2g}), Mo $4d$ (t_{2g}), and O $2p$ character at the Fermi level.

The SIC-LSD calculations find all the double perovskites studied to have half-metallic groundstate, with 100% spin-polarized conduction electrons [13]. The spin-polarized ground state densities of states (DOS) are very similar for all the compounds, independently of which alkaline earth compound is considered. In Figure 1 we show only the spin-polarized DOS for Sr_2FeMoO_6. The DOS show a convincing half-metallic behaviour, with well defined gap at the Fermi energy in the majority spin channel, and strongly hybridized Fe $3d$, Mo $4d$ and oxygen $2p$ states, in

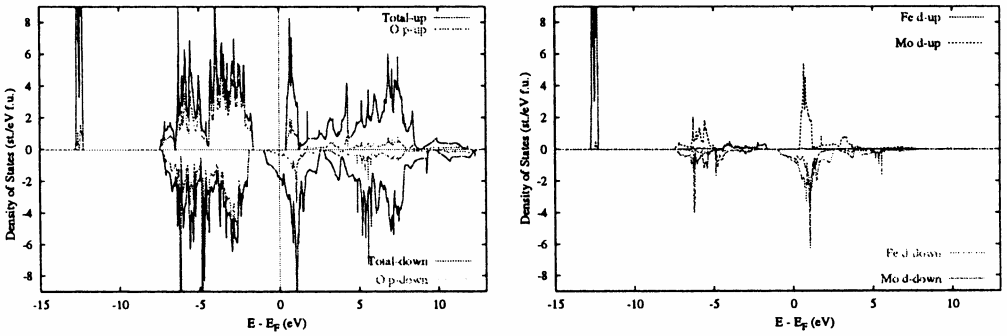

Fig. 1. Spin polarized total and oxygen $2p$ densities of states, per formula unit, for Sr_2FeMoO_6 (left), and spin polarized Fe $3d$ and Mo $4d$ densities of states per formula unit (right)

the other spin channel. In the ionic model for A_2FeMoO_6, where A = Ca, Sr, Ba, one would expect insulating behaviour due to the A^{2+}, Fe^{3+}, Mo^{5+}, and O^{2-} valencies. However, we obtain an Fe^{3+}/Mo^{6+} ground state configuration (namely five localized Fe d electrons and six delocalized Mo d electrons), meaning that while 12 electrons fill up the O holes in both the majority and minority spin channels, the remaining one electron will partially fill the conduction bands, unoccupied in the insulating scenario. Half-metallicity results from the fact that, due to Fe-Mo-O hybridization, the conduction bands are exchange split, and therefore the one electron occupies the minority conduction bands only.

In Table I, the half-metallic character is reflected through the total spin magnetic moments that are all integer. The spin moments induced by hybridization on the Mo sites of the various compounds are of similar magnitude, about $-0.4\ \mu_B$, independently of the alkaline earth element, while that of Re is of the order of $-1.1\ \mu_B$. These induced spin magnetic moments are antiparallel aligned with the Fe spin moment. It is interesting to note that the magnetic properties of these compounds seem unaffected by either the type of the alkaline earth atom, or the substantial change in their volumes. Also, the reduction in the size of the Fe and Mo spin moments for Sr_2FeMoO_6, as a result of implementing theoretical optimization of oxygen positions, as given by Kobayashi et al. [12], does not seem too important although brings the size of our calculated spin moments (given in parenthesis in the fourth column of Table I), close to their values. The changes in the spin moments of the other species cannot be resolved when rounded off to two digits after the decimal point.

Table I. Total and species decomposed spin magnetic moments (in μ_B) as calculated within SIC-LSD. In the last row the respective volumes per formula unit are quoted (in (atomic unit)^3)

Moment	Ca_2FeReO_6	Ca_2FeMoO_6	Sr_2FeMoO_6	Ba_2FeMoO_6
M_{total}	3.00	4.00	4.00 (4.00)	4.00
M_{Fe}	3.87	3.76	3.71 (3.65)	3.81
M_{Mo}	–	-0.40	-0.43 (-0.35)	-0.41
M_{Re}	-1.12	–	–	–
M_A	-0.02	0.01	0.02 (0.02)	0.02
M_{O1}	0.02	0.10	0.11 (0.11)	0.09
M_{O2}	0.01	0.11	0.11 (0.11)	–
M_{O3}	0.11	0.11	–	–
Volume	773.8	777.5	830.2	884.0

It follows from the SIC-LSD energy minimization that for the Mo-compounds, in the SIC-LSD calculations, the Fe^{3+} configuration has been most energetically favourable, followed by Fe^{4+} (energetically unfavourable by 53, 61 and 42 mRy per formula unit, in Ba-, Sr- and Ca-compounds, respectively), and Fe^{2+} configuration, at least twice as unfavourable as the former configuration (specifically, by 103, 122 and 125 mRy per formula unit). Moreover, treating also Mo *d* states as localized has been energetically unfavourable, and the more states have been considered as localized, the more unfavourable solutions have been obtained. In short, we obtain the nominal valencies of Fe^{3+} and Mo^{6+} in the ground state of all the Mo-double perovskites studied here.

Also for Ca_2FeReO_6 we find the groundstate to be half-metallic, rather than insulating [14]. The corresponding nominal valencies, Fe^{3+} and Re^{7+}, entail that in this case, 8 out of 14 electrons, fill the O *p* band in the minority spin channel plus some Fe and Re t_{2g} states. This is reflected in the total spin magnetic moment (Table I), which drops from 4 μ_B in Ca_2FeMoO_6 to 3 μ_B in Ca_2FeReO_6. Compared to the half-metallic groundstate, the SIC-LSD insulating states found for Ca_2FeReO_6, when treating six Fe 3*d* electrons (Fe^{2+}) and one Re 5*d* electron (Re^{6+}) as localized, have been unfavourable by about 195-235 mRy/formula unit, depending on the symmetry of the localized states. Also, the insulating and nearly insulating states, obtained for the cases where five majority Fe 3*d* (Fe^{3+}) electrons and two minority Re 5*d* (Re^{5+}) electrons have been treated as localized, have been unfavourable respectively by 140 and 170 mRy per formula unit, with respect to the calculated half-metallic groundstate of this compound. The reason being that the loss in band formation energy upon localization of Re *d* electrons by far outweighs the gain in localization energy. In summary, the half-metallic ground state seems to be a rather generic result for the double perovskites involving Fe with filled majority *d* shell, filled O *p* band, and Mo and Re transition metal ions which see their minority *d* bands occupied by one (Mo) to two (Re) electrons.

3. 2. Magnetite

Based upon its high magnetoresistive properties, magnetite (Fe_3O_4) is also of interest for technological applications, as e.g. computer memory, magnetic recording, etc. Magnetite is thought to be half-metallic, with a highest known T_c of 860 K. Remarkably, at about T_V = 122 K it undergoes a transition to an insulating state, associated with some kind of charge order, setting in on the octahedral sites, and a distortion of the crystal structure from the inverse spinel cubic

to monoclinic [15, 16]. Verwey argued that below the transition temperature, T_V, the Fe^{3+} and Fe^{2+} cations order in the alternate (001) planes, and interpreted this transition as an electron localization-delocalization transition [15].

To study charge order in magnetite, we have considered three different arrangements of Fe's on the octahedral sites, namely the simple Verwey order (SIC(1)), the case where all the octahedral sites are occupied by Fe^{3+} (SIC(2)), and finally the scenario with all the octahedral sites occupied by the Fe^{2+} ions (SIC(3)) [17]. For all these scenarios the tetrahedral sites have been occupied only by Fe^{3+}.

Table II. Total and type-decomposed spin magnetic moments (in Bohr magnetons μ_B) for LSD and three different SIC-LSD scenarios for the cubic structure, with only different Fe types listed. In the LSD, SIC(2) and SIC(3) calculations there is only one type of octahedral sites ($B1 \equiv B2 \equiv B$). Also given are the total energy differences (in mRy/formula unit) with respect to the ground state configuration. These energy differences are further decomposed into the energy loss in band formation/hybridization (ΔE_{BF}) and the energy gain due to localization (ΔE_{SIC}), both relatively to the respective energies of the ground state configuration

Scenario	M_{total}	$M_{Fe,t}$	$M_{Fe_{B1}}$	$M_{Fe_{B2}}$	ΔE	ΔE_{BF}	ΔE_{SIC}
LSD	4.00	3.40	-3.57	-3.57	894	-118	1012
SIC (1)	4.00	4.00	-3.57	-4.08	113	168	-55
SIC (2)	4.00	4.02	-3.90	-3.90	0	0	0
SIC (3)	2.00	4.01	-3.47	-3.47	374	475	-101

Our total energy calculations, both for the cubic (high temperature) – Table II and monoclinic (low temperature) structures, show that not the Verwey phase, but the scenario with all interstitial sites occupied by Fe^{3+}, is the ground state, followed by the Verwey phase (unfavourable by 113 mRy), and then the all Fe^{2+} scenario (unfavourable by 374 mRy). The way this comes about is due to the competition between the band formation/hybridization energy, ΔE_{BF}, and the localization energy, ΔE_{SIC}, as seen in Table II for the cubic phase. Whilst the localization energy favours more localized states, and hence the formation of Fe^{2+} on half of the octahedral sites (SIC(1) scenario), the corresponding loss of band formation energy by three times outweighs the gain in localization energy. The significant total energy difference, ΔE, of 113 mRy per formula unit (108 mRy for monoclinic phase), found between the scenario SIC(1) and scenario SIC(2), renders the simple Verwey ordering highly unlikely as an explanation for the properties in the low temperature phase of magnetite. Thus, we conclude that, if at all, the charge order must be much more complex than postulated by Verwey. In the Verwey phase, we have calculated magnetite to be insulating with a gap of ~0.35 eV in cubic phase (~0.1 eV in monoclinic phase), while the all Fe^{3+} scenario, depending on structure, has given rise to half-metallic or metallic (with a very high spin polarization) solution [17].

Let us now comment briefly on the spin resolved charges of various Fe sites. The tetrahedral Fe sites are found to be very much the same for all different scenarios except for the LSD. The situation is different for the octahedral sites. In particular, in the Verwey charge ordered scenario, the different octahedral ions show similar numbers in one spin component ($Fe_{B1}\downarrow = 5.81$, *vs.* $Fe_{B2}\downarrow = 5.90$), but differ by about 0.42 electron in the other spin component ($Fe_{B1}\uparrow = 2.24$, *vs.* $Fe_{B2}\uparrow = 1.82$) of the cubic structure, which is due to localization of the sixth *d* electron. So, while in the ionic picture the valence of the two different octahedral sites (*B*1 and *B*2) differs by one, in

terms of the charge disproportionation they are only 0.32 electron different, in line with experiments. It is important to note, that even for the all trivalent ground state configuration in the monoclinic structure, we find charge disproportionation of between 0.2 to 0.36 electron, for the octahedral sites. These calculated charge disproportionations are in better agreement with the recent experimental study by Wright et al. [18] than the ones of the Verwey charge ordered phase.

Obviously we have managed to study only the three simplest charge order scenarios, and within these restrictions our results indicate the energetically unfavourable character of Fe^{2+}. Our work has shown that the SIC-LSD is capable to study any kind of static charge order, although realization of more complicated charge arrangements, which might be of relevance to future studies, may be limited by memory and CPU of present computers. Given these limitations that we only studied a simple Verwey charge ordered state, we have concluded that the charge disproportionation below the Verwey temperature is structural in origin and all Fe ions occur in a trivalent state. This does not exclude the possibility that Fe_3O_4 below the Verwey temperature is described by a much more complicated charge ordered state.

3. 3. Vacancy doped transition metal oxides

Recently, it has been predicted [19] that nonmagnetic insulating oxides, like CaO and MgO, in the rocksalt-structure, can be made half-metallic upon introduction of a low concentration of vacancies on the cation sites. Here we show, based on first-principles SIC-LSD calculations, that introducing cation vacancies into antiferromagnetic insulating transition-metal (TM) oxides not only leads to half-metallic behaviour, but in NiO a half-metallic antiferromagnetic state can be realised [6].

We have performed *ab initio* calculations using a supercell approach to simulate the effect of placing vacancies in MnO and NiO [6]. The cubic supercell used in the calculations comprises 32 formula units. To gain more insight, we have studied in addition to the experimentally observed AF2 ordering also a ferromagnetic (FM) aligmnent of spins. For the systems without vacancies, we have observed for both oxides insulating behaviour, with large band gaps at the Fermi energy. The gaps are of charge transfer type – the top of the valence band is predominantly oxygen *p*-like, whereas the bottom of the conduction band is formed by transition-metal *d*-states. The oxygen *p* bands are not polarized in these AF2 bulk materials (see also [9]). For 3.125% of vacancies, introduced onto one spin sublattice (realizing $Mn_{0.97}O$ and $Ni_{0.97}O$), our calculations give half-metallic behaviour for both antiferromagnetic (AF2) and ferromagnetic (FM) orders.

Table III. Total spin magnetic moments of the supercell with and without vacancy. IS and HM denote insulating and half-metallic states, respectively

System	Scenario	m^{total} (in μ_B)	State
MnO	AF2 no vacancy	0	IS
	AF2 with vacancy	3	HM
NiO	AF2 no vacancy	0	IS
	AF2 with vacancy	0	HM

Table III shows the total spin magnetic moments of MnO and NiO without and with vacancies as calculated in the SIC-LSD supercell approach. In all the cases we obtain integer total spin magnetic moments. Most interestingly, a cation vacancy embedded into AF2-ordered NiO gives total spin magnetic moment of zero, i.e., this system is a half-metallic antiferromagnet [4]. The spin moments given in Table III imply that the spin polarization of neighbouring atoms, induced by vacancy creation, gives rise to a compensating integer spin moment of 2 μ_B, which in the case of NiO in the AF2 ordering, makes the total spin moment exactly zero μ_B.

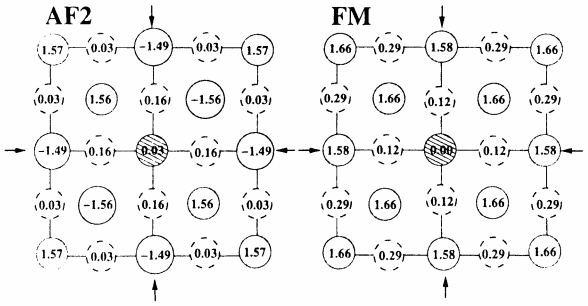

Fig. 2. Spin magnetic moments in the (100)-plane of $Ni_{0.97}O$. The underlying pattern of the supercell is AF2 and FM (right panel). The respective spin moments of NiO without vacancy are $m_{Ni}^{AF2} = \pm 1.56\ \mu_B$, $m_O^{AF2} = 0\ \mu_B$, $m_{Ni}^{FM} = 1.66\ \mu_B$, $m_O^{FM} = 0.34\ \mu_B$. Small arrows indicate the positions of next nearest neighbours to the impurity

A more detailed look at the distribution of spin moments around the vacancy for the case of NiO (the findings for MnO are similar) is displayed in Fig. 2 (left panel), where we show the spin magnetic moments in the ASA spheres in the (100) plane in the neighbourhood of the vacancy. As can be seen for the case of an underlying AF2 ordering, the oxygens around the vacancy acquire a spin moment of $0.16\mu_B$ (in the system without vacancy the oxygens are frustrated in the AF2 ordering and have no spin moment), thus restoring the AF2 pattern, disturbed by taking out the Ni atom at the vacancy site. When comparing the spin moments on the Ni spheres to the respective bulk value of $\pm 1.56\mu_B$, one realises that the nearest Ni-neighbours to the vacancy are essentially unaffected. However, the spin moments on the Ni next-nearest neighbours are decreased in magnitude by 0.07 μ_B. This is a result of the fact that the Anderson exchange *via* oxygen, which we miss out at the site of the vacancy, plays a dominant role over the ninety degree exchange to nearest neighbours. This is also reflected through the change of other quantities, e.g. the change of calculated charges in the ASA spheres. Adding up the spin magnetic moments of the spheres over the whole unit cell gives zero total spin magnetic moment. The compensating spin moment of 2 μ_B for the Ni-cation taken out is mainly distributed over the oxygens surrounding the vacancy and the Ni atoms being the next-nearest neighbours to the vacancy (marked by arrows in Fig. 2). The same is observed in the case of an underlying FM ordering (Fig. 2, right panel), where the compensation of 2 μ_B reveals itself through the reduction of the spin moments both on the oxygens surrounding the vacancy and the next-nearest neighbour cations, as compared to the system without vacancy.

The vacancy induced half-metallicity of TM oxides survives a local 10% inward relaxation of the neighbouring oxygen atoms, but is lost when doubling the vacancy concentration on the same sublattice. The situation is the same when one removes a cation from each sublattice at the same time. In the present supercell approach this means that the two cation vacancies are

placed so that both see the same environment, however with a reversed spin ordering. In this scenario, the half-metallicity is lost when considering the global picture, however, the spin-polarization persists locally. Thus, if this local spin-polarization was present at the surface, it could be detected by SPSTM.

4. CONCLUSIONS

We have shown that, owing to a better treatment of correlations, SIC-LSD can provide useful insight to the nature of a variety of half-metallic oxides. One can not only study their electronic and magnetic properties, but also such issues as valence and charge order. In particular, we have studied half metals obtained by both electron and hole doping. The latter has been realized in the vacancy induced $Ni_{0.97}O$ and $Mn_{0.97}O$, where the carriers are predominantly O p, while the former occurs in the double perovskites and magnetite, where the carriers are mostly transition metal d electrons. Thus, it has been shown that SIC-LSD is a valuable tool for describing these new half metals of high technological importance.

Acknowledgements

This work has been partially funded by Research Training Network "Computational Magnetoelectronics" (contract: HPRN-CT-2000-00143). Work of L. Petit has been supported by the Defence Advanced Research Project Agency and by the Division of Materials Science and Engineering, US Department of Energy, under Contract No. DE-AC05-00OR22725 with UT-Battelle LLC. Work of G. M. Stocks has been supported by US, DOE-OS, BES-DMSE under contract number DE-AC05-00OR22725 with UT-Battelle LLC. Part of the calculations for Fe_3O_4 has been performed at CCS-ORNL and NERSC. Computational work at CCS has been supported by OASCR-MICS.

References

[1] R. A. de Groot, F. M. Mueller, P.G. van Engen, K. H. J. Buschow, Phys. Rev. Lett. **50**, 2024 (1983).
[2] J. M. D. Coey and M. Venkatesan, J. Appl. Phys., **91**, 8345 (2002).
[3] H. Eschrig and W. E. Pickett, Solid State Commun., **118**, 123 (2001).
[4] H. van Leuken and R. A. de Groot, Phys. Rev. Lett., **77**, 1171 (1995).
[5] W. E. Pickett, Phys. Rev. Lett., **77**, 3185 (1996).
[6] D. Ködderitzsch, W. Hergert. Z. Szotek, W. M. Temmerman, Phys. Rev. **B68**, 125114 (2003).
[7] W. M. Temmerman, A. Svane, Z. Szotek, H. Winter, in: *Electronic Density Functional Theory: Recent, Progress and New Directions*, eds. J. F. Dobson, G. Vignale, M. P. Das, Plenum Press, New York and London, 1998.
[8] A. Svane and O. Gunnarsson, Phys. Rev. Lett., **65**, 1148 (1990).
[9] Z. Szotek, W. M. Temmerman, H. Winter, Phys. Rev., **B47**, 4029 (1993).
[10] P. Strange, A. Svane, W. M. Temmerman, Z. Szotek, H. Winter, Nature, **399**, 756 (1999).
[11] J. P. Perdew and A. Zunger, Phys. Rev., **B23**, 5048 (1981).
[12] K. -I. Kobayashi, T. Kimura, H. Sawada, K. Terakura, Y. Tokura, Nature, **395**, 677 (1998); Phys. Rev., **B59**, 11159 (1999).
[13] Z. Szotek, W. M. Temmerman, A. Svane, L. Petit, H. Winter, Phys. Rev. B (2003).
[14] J. Gopalakrishnan, A. Chattopadhyay, S. B. Ogale, T. Venkatesan, R. L. Greene, A. J. Millis, K. Ramesha, B. Hannoyer, G. Marest, Phys. Rev., **B62**, 9538 (2000).
[15] E. J. W. Verwey and P. W. Haayman, Physica (Utrecht), **8**, 979 (1941); E. J. W. Verwey, P. W. Haayman, F. C. Romeijan, J. Chem. Phys., **15**, 181 (1947).
[16] F. Walz, J. Phys.: Condens. Matter, **14**, R285 (2002).
[17] Z. Szotek. W. M. Temmerman, A. Svane, L. Petit, G. M. Stocks, H. Winter, Phys. Rev. **B68**, 054415 (2003).
[18] J. P. Wright, J. P. Attfield, P. G. Radaelli, Phys. Rev. Lett., **87**, 266401 (2001).
[19] I. S. Elfimov, S. Yunoki, G. A. Sawatzky, Phys. Rev. Lett., **89**, 216403 (2002).